

[see commentary on page 247](#)

Reduction of anionic sites in the glomerular basement membrane by heparanase does not lead to proteinuria

MJ van den Hoven¹, TJ Wijnhoven^{2,3}, J-P Li⁴, E Zcharia⁵, HB Dijkman⁶, RG Wismans², AL Rops¹, JF Lensen², LP van den Heuvel³, TH van Kuppevelt², I Vlodavsky⁷, JHM Berden¹ and J van der Vlag¹

¹Nephrology Research Laboratory, Department of Nephrology, Nijmegen Centre for Molecular Life Sciences, Radboud University Nijmegen Medical Centre, Nijmegen, The Netherlands; ²Department of Matrix Biochemistry, Nijmegen Centre for Molecular Life Sciences, Radboud University Nijmegen Medical Centre, Nijmegen, The Netherlands; ³Department of Pediatric Nephrology, Radboud University Nijmegen Medical Centre, Nijmegen, The Netherlands; ⁴Department of Medical Biochemistry and Microbiology, Biomedical Center Uppsala University, Uppsala, Sweden; ⁵Department of Oncology, Hadassah-Hebrew University Medical Center, Jerusalem, Israel; ⁶Department of Pathology, Radboud University Nijmegen Medical Centre, Nijmegen, The Netherlands and ⁷Cancer and Vascular Biology Research Center, Rappaport Faculty of Medicine, Technion, Haifa, Israel

Heparan sulfate in the glomerular basement membrane has been considered crucial for charge-selective filtration. In many proteinuric diseases, increased glomerular expression of heparanase is associated with decreased heparan sulfate. Here, we used mice overexpressing heparanase and evaluated the expression of different heparan sulfate domains in the kidney and other tissues measured with anti-heparan sulfate antibodies. Glycosaminoglycan-associated anionic sites were visualized by the cationic dye cupromeronic blue. Transgenic mice showed a differential loss of heparan sulfate domains in several tissues. An unmodified and a sulfated heparan sulfate domain resisted heparanase action *in vivo* and *in vitro*. Glycosaminoglycan-associated anionic sites were reduced about fivefold in the glomerular basement membrane of transgenic mice, whereas glomerular ultrastructure and renal function remained normal. Heparanase-resistant heparan sulfate domains may represent remnant chains or chains not susceptible to cleavage. Importantly, the strong reduction of glycosaminoglycan-associated anionic sites in the glomerular basement membrane without development of a clear renal phenotype questions the primary role of heparan sulfate in charge-selective filtration. We cannot, however, exclude that overexpression of heparanase and heparan sulfate loss in the basement membrane in glomerular diseases contributes to proteinuria.

Kidney International (2008) **73**, 278–287; doi:10.1038/sj.ki.5002706; published online 28 November 2007

KEYWORDS: transgenic mouse; glomerular filtration barrier; renal function

Correspondence: J van der Vlag, Nephrology Research Laboratory (279), Department of Nephrology, Nijmegen Centre for Molecular Life Sciences, Radboud University Nijmegen Medical Centre, Geert Grooteplein 26-28, Nijmegen 6525 GA, The Netherlands. E-mail: J.vanderVlag@NIER.UMCN.NL

Received 18 April 2007; revised 28 September 2007; accepted 9 October 2007; published online 28 November 2007

Heparan sulfate proteoglycans are expressed at the surface of virtually all cells and in the extracellular matrix. Heparan sulfate proteoglycans consist of a core protein with linear covalently attached heparan sulfate (HS) sugar side chains that belong to the family of strong negatively charged glycosaminoglycans that also includes heparin and non-sulfated hyaluronan. The HS chain comprises up to 150 $\alpha(1\text{--}4)$ -glucuronate- $\beta(1\text{--}4)$ -N-acetyl-glucosamine disaccharide units that can be modified extensively. Modifications of HS include N-deacetylation/N-sulfation of N-acetylglucosamine; C-5 epimerization of glucuronic acid to iduronic acid; and 2-O-, 3-O-, and 6-O-sulfation. The structure of the HS chains may be edited by HS-modifying enzymes that include heparanase, a $\beta(1\text{--}4)$ -endoglucuronidase that cleaves HS at specific sites, and HS 6-O-endosulfatases that specifically remove 6-O-sulfate. The combination of possible modifications gives rise to an enormous structural diversity of the HS chain, which dictates the binding and modulation of a myriad of factors that include growth factors, chemokines, cytokines, enzymes, and structural proteins. These HS-bound factors are key mediators in many biological and pathological processes.^{1,2}

For several decades, it has been hypothesized that the negatively charged HS in the glomerular basement membrane (GBM) is crucial for the charge-selective permeability of the glomerular capillary filter. Seminal studies by Farquhar, Kanwar, and co-workers demonstrated the presence of glycosaminoglycans, including HS, in the GBM, whereas removal of glycosaminoglycans in the GBM by perfusion of bacterial glycosaminoglycan-degrading enzymes led to the passage of ferritin and labeled bovine serum albumin through the GBM.^{3–6} Furthermore, the injection of anti-heparan sulfate proteoglycan antibodies led to albuminuria in rats.^{7,8} Finally, in many experimental and human glomerular diseases, such as diabetic nephropathy, minimal

change disease, and membranous glomerulopathy, a decreased expression of HS in the GBM was observed when probed with our monoclonal anti-HS antibody JM403,^{9–13} which in general correlated with the level of urinary protein excretion. In contrast to HS, the expression of agrin, the HS proteoglycan core protein most abundantly present in the GBM,¹⁴ was not altered. In recent years it became evident that the decreased expression of HS in the GBM in several human and experimental proteinuric diseases could be attributed to an increased glomerular expression of heparanase.^{15–21} However, we showed that intravenous injection of the bacterial HS-degrading enzyme heparinase III in rats resulted in a near complete loss of anionic sites in the GBM without the development of proteinuria within 48 h.²² This finding challenged the primary role of HS in the GBM in charge-selective filtration.

Mammalian heparanase is synthesized as a 68-kDa pre-proheparanase protein. After cleavage of an N-terminal signal peptide, the latent proheparanase protein of 65 kDa is formed, which has no enzymatic activity. The proheparanase protein is proteolytically processed by cathepsin L in endosomes/lysosomes, which yields an active heterodimer consisting of a 8-kDa N-terminal subunit and a 50-kDa C-terminal subunit.^{23,24} Cleavage of HS chains by heparanase occurs at a few selective sites within a HS chain. Heparanase cleaves the $\beta(1-4)$ bond within HS, which requires *N*- and 6-*O*-sulfated moieties in a specific context as exemplified in the trisaccharide sequence GlcNS6OS- $\alpha(1-4)$ -GlcA- $\beta(1-4)$ -GlcNS6OS.^{25,26} The role of heparanase in metastasis, angiogenesis, and inflammation has been well-established.²³ Recently, we generated transgenic mice overexpressing human heparanase (HPSE-tg).²⁷ A first inventory of HPSE-tg mice showed a very mild proteinuria compared with controls. In the current study we analyzed the expression of different HS domains, in particular in the kidney, in both HPSE-tg and control mice of up to 8 months old by probing with specific anti-HS antibodies. Furthermore, we determined the presence of glycosaminoglycan-associated anionic sites in the GBM by probing with the cationic dye cupromeronic blue. Finally, we evaluated glomerular ultra-structure and renal function.

RESULTS

Renal overexpression of human heparanase in HPSE-tg mice

The expression of mammalian heparanase in kidneys from HPSE-tg and control mice was evaluated (Figure 1), which exclusively revealed mRNA (Figure 1a) and protein (Figure 1b) expression of human heparanase in HPSE-tg mice. Both the latent 65-kDa proheparanase protein and the 50-kDa subunit of active heparanase could be detected, whereas the 50-kDa protein was more abundantly expressed (Figure 1b). Immunofluorescence staining of renal sections revealed the expression of the human heparanase protein in both tubuli and glomeruli of HPSE-tg mice (Figure 1c).

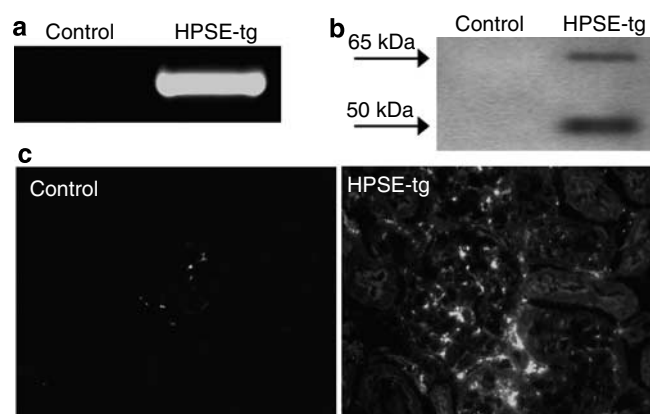


Figure 1 | Renal overexpression of human heparanase in HPSE-tg mice. (a) Heparanase mRNA expression analysis revealed a high human heparanase mRNA expression in the kidney of HPSE-tg mice, whereas no expression was observed in controls. (b) Western blot analysis of kidney tissue lysates showed that both the latent 65-kDa heparanase and the processed 50-kDa heparanase are expressed in HPSE-tg mice but not in controls. (c) Immunofluorescence staining demonstrated that heparanase is overexpressed in both glomeruli and tubuli of HPSE-tg mice compared to controls. Original magnification $\times 40$.

Differential loss of distinct HS domains in HPSE-tg and control mice

The expression of different HS domains in renal sections of HPSE-tg and control mice was evaluated by probing with specific anti-HS antibodies. We applied the monoclonal antibody NAH46 recognizing *N*-acetylated unmodified HS domains, which resembles the structure of the bacterial polysaccharide K5,²⁸ the monoclonal antibody JM403 recognizing HS domains containing *N*-unsubstituted glucosamine residues,²⁹ and phage display-derived single-chain antibodies recognizing sulfated HS domains (Table 1; Figure 2). HS domains containing *N*-unsubstituted glucosamine residues probed with JM403 were completely absent in kidneys of HPSE-tg mice (Figure 2b) compared with controls (Figure 2a). Note the loss of staining by JM403 along the capillary wall in the GBM of HPSE-tg mice. In contrast, the expression of *N*-acetylated unmodified HS domains probed with NAH46, in different renal structures including the GBM, was not different between control (Figure 2c) and HPSE-tg mice (Figure 2d). There was a moderate to strong expression of sulfated HS domains in the GBM of controls probed with HS4C3, EV3B2, HS3A8, and AO4B08 (Figure 2e, g, i, and k). The expression of these sulfated HS domains in the GBM of HPSE-tg mice was either strongly decreased (HS4C3; Figure 2f) or lost (EV3B2 and HS3A8; Figure 2h and j), whereas the expression of the sulfated HS domain defined by AO4B08 persisted (Figure 2l). The sulfated HS domains defined by HS4E4 and LKIV69 that are not located in the GBM of controls (Figure 2m and o), were also lost in HPSE-tg mice (Figure 2n and p). An increased glomerular dermatan sulfate or chondroitin sulfate (CS) expression could serve as potential compensatory mechanisms for the loss of HS in the GBM of HPSE-tg mice. Analysis with

Table 1 | Antibodies used in this study

Antibody	Antibody isotype	Preferred epitopes	Source or reference
JM403	Monoclonal mouse IgM	Anti-HS: GlcN	van den Born <i>et al.</i> ^{8,29}
NAH46	Monoclonal mouse IgM	Anti-HS: GlcNAc-GlcA	Seikagaku, Tokyo, Japan
AO4B08	ScFv	Anti-HS: GlcNS6S-IdoA2S	Jenniskens <i>et al.</i> , ³⁰ Kurup <i>et al.</i> ³¹
EV3B2	ScFv	Anti-HS: GlcNS ± 6S-GlcA/IdoA	Dennissen <i>et al.</i> ³²
HS3A8	ScFv	Anti-HS: GlcNS6S-IdoA2S	Dennissen <i>et al.</i> ³²
HS4C3	ScFv	Anti-HS: GlcNS3S6S-GlcA/IdoA2S	van Kuppevelt <i>et al.</i> ³³
HS4E4	ScFv	Anti-HS: GlcNAc/GlcNS-IdoA	Dennissen <i>et al.</i> , ³² Kurup <i>et al.</i> ³¹
LKIV69	ScFv	Anti-HS: GlcNS-IdoA2S	Wijnhoven <i>et al.</i> ³⁴
IO3H10	ScFv	Anti-CS A, C, and E:	Smetsers <i>et al.</i> ³⁵
HPA1	Rabbit IgG	Anti-human heparanase	ProsPecTany, Rehovot, Israel
MI91	Monoclonal hamster IgG	Anti-agrin, N-terminus	Raats <i>et al.</i> ¹⁴

CS A, C, and E, chondroitin sulfate A, C, and E; GlcA, D-glucuronic acid; GlcN, N-unsubstituted glucosamine; GlcNS, N-sulfated glucosamine; HS, heparan sulfate; IdoA, L-iduronic acid; 2S, 2-O-sulfated; 3S, 3-O-sulfated; 6S, 6-O-sulfated; ScFv, single-chain variable fragment antibody.

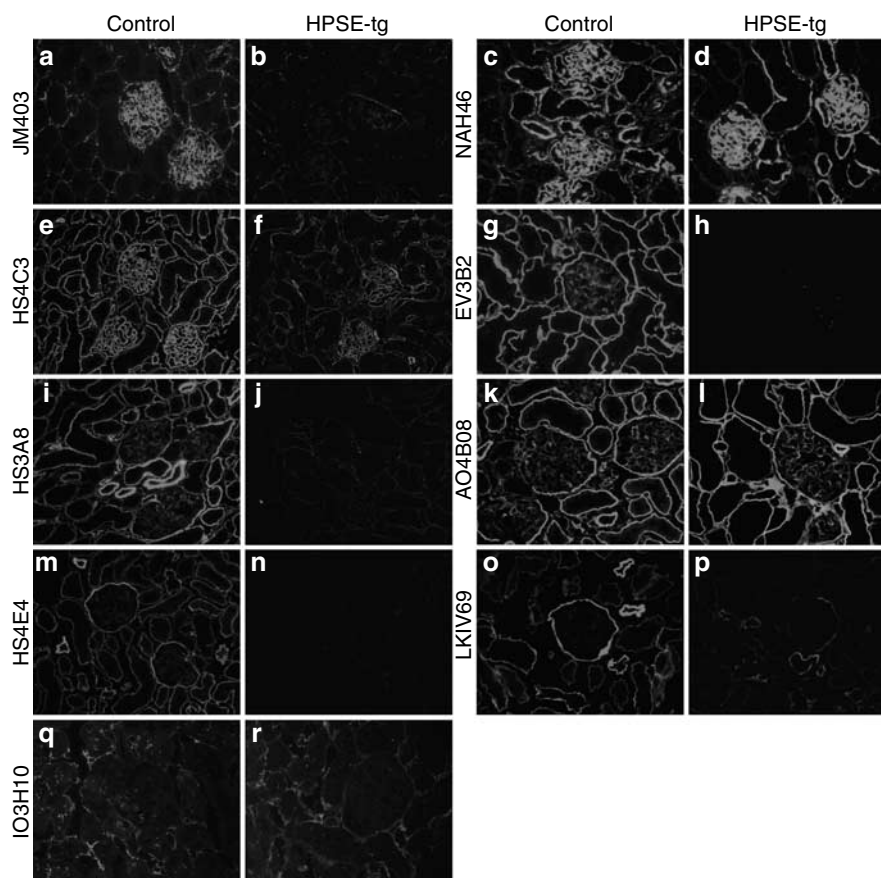


Figure 2 | Transgenic overexpression of heparanase in HPSE-tg mice leads to differential loss of HS domains. Expression of HS domains with N-unsubstituted glucosamine residues is especially found in the GBM of controls, as probed with antibody JM403 (a), whereas no expression could be detected in the glomeruli of HPSE-tg mice (b). However, expression of unmodified N-acetylated HS domains in the GBM, recognized by antibody NAH46, was similar in controls and HPSE-tg mice (c, d). There was a moderate to strong expression of sulfated HS domains in the GBM of control kidneys, as probed with HS4C3, EV3B2, HS3A8, and AO4B08 (e, g, i, k). Expression of the sulfated HS domains in the GBM of HPSE-tg mice was either strongly reduced (HS4C3) (f) or abolished (EV3B2 and HS3A8) (h, j), whereas expression of the sulfated HS domains recognized by AO4B08 in the GBM of HPSE-tg mice was normal (l). Expression of sulfated HS domains that are not located in the GBM of controls, but mainly in the Bowman's capsule and tubular basement membrane (HS4E4 and LKIV69) (m, o) was also absent in HPSE-tg mice (n, p). Glomerular expression of CS, which could serve as a compensatory mechanism for the glomerular loss of HS in HPSE-tg mice, was hardly detectable in controls (q) and not increased in HPSE-tg mice (r). See also Table 2 for a summary of the expression of HS/CS domains in the kidney. Original magnification $\times 40$.

specific antibodies revealed no glomerular expression of dermatan sulfate in either HPSE-tg or control mice (data not shown), while probing for CS with the anti-CS antibody IO3H10 only revealed a hardly detectable glomerular staining,

which was similar for HPSE-tg mice and controls (Figure 2q and r), and in line with previous findings.³⁵ Table 2 summarizes the morphological expression of the different HS/CS domains in renal sections of HPSE-tg mice and controls.

Table 2 | Renal expression of distinct HS domains in HPSE-tg and controls as probed with anti-HS antibodies

	JM403		NAH46		HS4C3		EV3B2		HS3A8		AO4B08		HS4E4		LKIV69		IO3H10	
	Contr.	Htg	Contr.	Htg	Contr.	Htg	Contr.	Htg	Contr.	Htg	Contr.	Htg	Contr.	Htg	Contr.	Htg	Contr.	Htg
GBM	++	-	++	++	++	±	+	-	±	-	±	±	-	-	-	-	±	±
Mesangium	-	-	+	+	++	±	+	±	±	-	±	±	-	-	-	-	-	-
Bowman's capsule	±	-	+	+	+	-	++	-	+	-	++	++	+	-	++	±	++	++
TBM	±	-	+	+	++	±	++	-	++	-	++	++	+	-	+	-	++	++
PTC	-	-	+	+	++	±	++	-	++	+	+	+	-	-	-	-	++	++
Blood vessels	-	-	+	+	+	-	+	-	++	-	-	-	+	-	++	-	+	+

Contr., control mice; GBM, glomerular basement membrane; HS, heparan sulfate; Htg, HPSE-tg mice; PTC, peritubular capillaries; TBM, tubular basement membrane; ++, strong staining; +, good staining; ±, moderate staining; and -, absent.

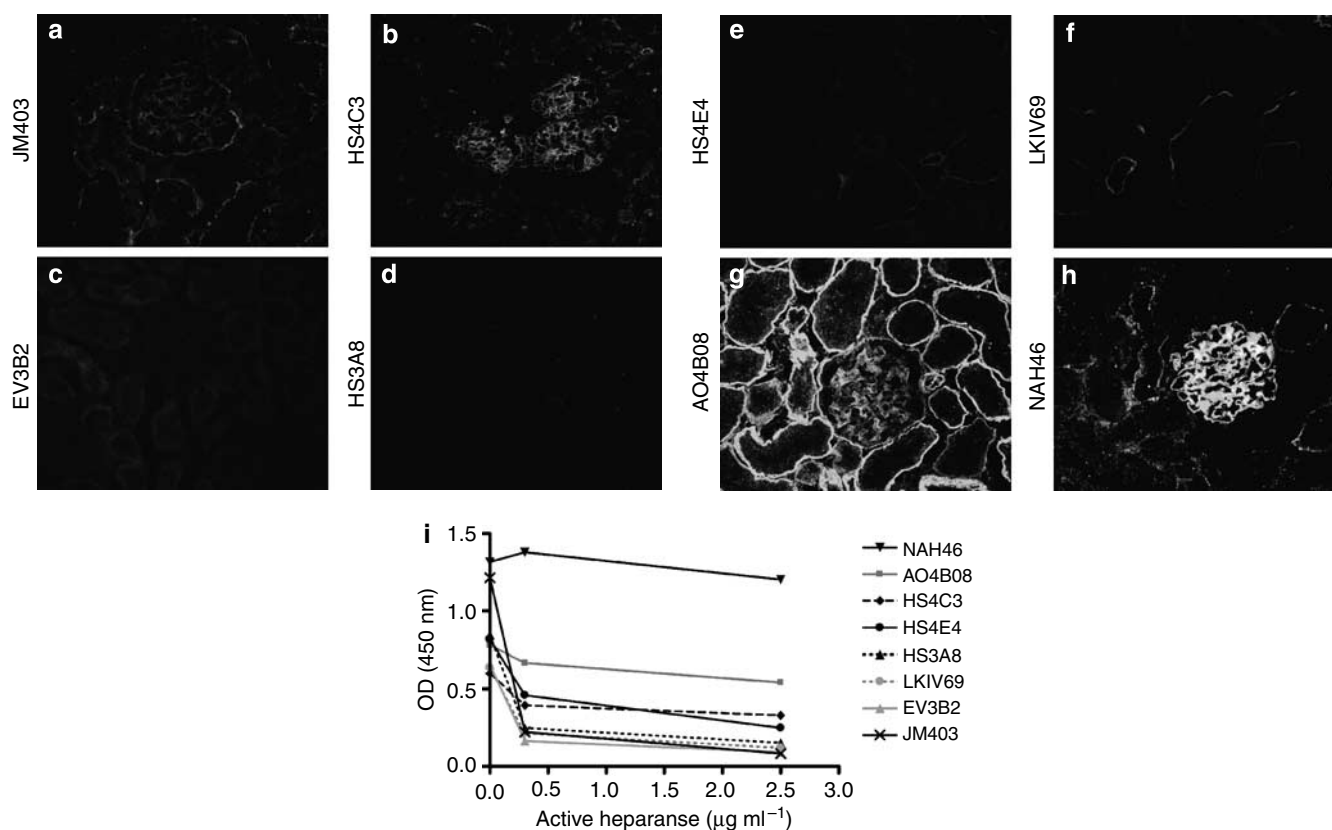


Figure 3 | Treatment of normal mouse kidney sections or coated HS with recombinant active heparanase leads to differential loss of HS domains. Expression of *N*-unsubstituted HS domains, probed with JM403 (a) and the highly sulfated HS domains, probed with HS4C3, EV3B2, HS3A8, HS4E4, and LKIV69 (b-f), was either strongly decreased or lost after heparanase treatment. Expression of the sulfated HS domain defined by AO4B08 (g) and the unmodified *N*-acetylated HS domain defined by NAH46 (h) persisted after exposure to heparanase. Note that the differential loss of HS domains was comparable to the patterns of HS expression in HPSE-tg mice (compare with Figure 2 a-p). (i) HS of bovine kidney coated in microtiter plates exposed to recombinant active heparanase at 0.3 or 2.5 µg ml⁻¹ for 3 h also revealed a differential loss of HS domains. At 2.5 µg ml⁻¹ a 93% decrease of the HS domain containing *N*-unsubstituted glucosamine residues defined by JM403 and a 70–86% decrease for the sulfated HS domains defined by EV3B2, HS3A8, HS4E4, and LKIV69 can be calculated. The sulfated HS domain defined by HS4C3 was reduced 45%, whereas the sulfated HS domain defined by AO4B08 was reduced 31%, and the *N*-acetylated unmodified HS domain defined by NAH46 was reduced 9%. Original magnification × 40.

The differential loss of HS domains in renal sections of HPSE-tg mice could be explained by locally different concentrations of active mammalian heparanase. Therefore, we treated renal sections of normal mice with active recombinant human heparanase. Probing of heparanase-treated renal sections with anti-HS antibodies revealed essentially the same differential loss of HS domains as observed in HPSE-tg

mice (Figure 3). The HS domain containing *N*-unsubstituted glucosamine residues defined by JM403, and the sulfated HS domains defined by HS4C3, EV3B2, HS3A8, HS4E4, and LKIV69, were either strongly decreased or completely lost (Figure 3a-f). In contrast, the sulfated HS domain defined by AO4B08 and the *N*-acetylated unmodified HS domain defined by NAH46, resisted heparanase treatment (Figure

3g and h). Finally, we treated HS from bovine kidney, coated in microtiter plates, with active mammalian heparanase at two concentrations followed by probing with anti-HS antibodies. This experiment confirmed the results obtained *in vivo* in the HPSE-tg mice and *in vitro* on renal sections of normal mice treated with active mammalian heparanase (Figure 3i). The HS domains in enzyme-linked immunosorbent assay after treatment with heparanase, as defined by the anti-HS antibodies, persisted in the following order NAH46 > AO4B08 > HS4C3 > HS4E4 > LKIV69 > HS3A8 > EV3B2 > JM403. Note that although in enzyme-linked immunosorbent assay binding of AO4B08 decreased more (31%) than that of NAH46 (9%), the binding of AO4B08 to tubular basement membranes after HPSE digestion was still stronger compared with NAH46. This can be explained by the fact that the staining of AO4B08 to tubular basement membranes of control sections was already much stronger than for NAH46.

Treatment of renal sections of HPSE-tg and control mice, and treatment of coated HS, with the bacterial HS-degrading enzyme heparinase III, resulted in the loss of all HS domains (data not shown).

In addition to renal sections, we evaluated the expression of HS domains in sections of spleen and liver of HPSE-tg and control mice. This revealed similar data as obtained for the kidney (data not shown).

In summary, overexpression of mammalian heparanase leads to a differential loss of HS domains in the GBM, which is similar for different tissues.

Loss of glycosaminoglycan-associated anionic sites in the GBM does not lead to a clear renal phenotype

In addition to the analysis with anti-HS antibodies, we visualized the number of glycosaminoglycan-associated anionic sites in the GBM of HPSE-tg and control mice, by probing with the cationic dye cupromeronic blue³⁶ (Figure 4). As expected, cupromeronic blue stained the GBM of controls, which was most intense at the podocyte side as revealed by black dots (Figure 4a and b), whereas occasionally some residual cupromeronic blue staining was found in the GBM of HPSE-tg mice, mainly at the endothelial side (Figure 4c and d). Visual scoring of the number of black dots in the GBM on several sections revealed a ~5-fold reduction of the number of glycosaminoglycan-associated anionic sites in HPSE-tg mice compared with controls. To evaluate whether there was a difference in overall turnover of HS in HPSE-tg compared with control mice, we analyzed the presence of glycosaminoglycans in the urine. Glycosaminoglycans were present in the urine of 8/11 HPSE-tg mice and 4/8 control mice (data not shown). Since we did not observe intracellular accumulation of HS, this suggests that chronic overexpression of heparanase does not lead to an increased biosynthesis and urinary secretion of HS.

It has been assumed that the charge-selective properties of the capillary filter are dictated by the negatively charged HS in the GBM. Therefore, we measured urinary albumin and creatinine in HPSE-tg and control mice. It appeared that on

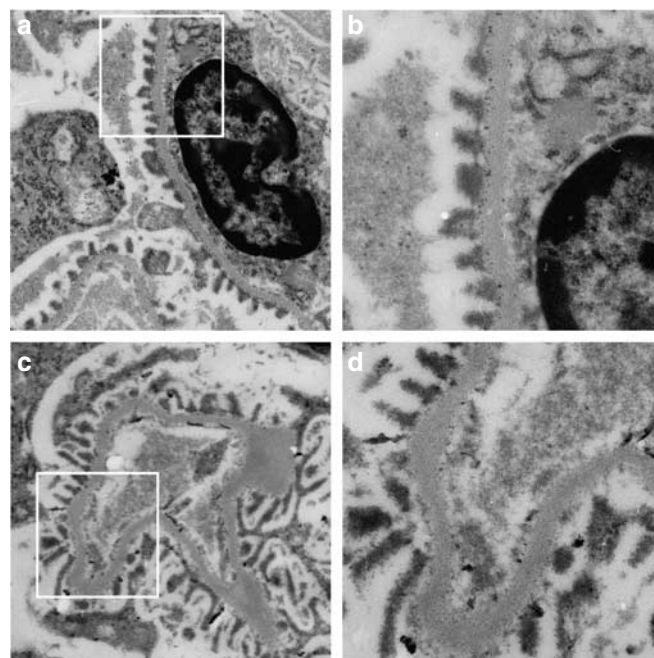


Figure 4 | Analysis of the number of glycosaminoglycan-associated anionic sites in the GBM of HPSE-tg and control mice. (a, b) Glycosaminoglycans, visualized by the cationic dye cupromeronic blue, were observed as a dotted-like pattern in the GBM of control mice, which was most intense at the side of the podocytes. (c, d) In the GBM of HPSE-tg mice, cupromeronic blue staining was strongly decreased, although occasionally some staining remained, mainly at the endothelial site of the GBM. Semiquantitative analysis (by counting the black dots per GBM surface area from 10 random sections of three individual mice of each mice strain) revealed a ~5-fold decreased binding of cupromeronic blue in the GBM of HPSE-tg mice compared with control mice. Original magnification $\times 10\,000$ (a, c); original magnification $\times 20\,000$ (b, d).

average the HPSE-tg mice ($n=11$) showed a low, but statistically significant higher level of albuminuria compared with controls ($n=9$), although the majority of HPSE-tg mice had urinary albumin/creatinine ratios within the normal range (Figure 5). Renal function, as measured by the concentration of serum creatinine, did not significantly differ between HPSE-tg mice ($22.5\,\mu\text{M} \pm 1.8$) and controls ($21.5\,\mu\text{M} \pm 1.5$) as found previously.²⁷ Finally, we examined the glomerular ultrastructure of HPSE-tg ($n=6$) mice and controls ($n=4$) (Figure 6). No differences could be observed between controls (Figure 6a and b) and HPSE-tg mice (Figure 6c and d). The appearance of GBM thickness, podocyte foot processes architecture, glomerular endothelium, and mesangium was similar for HPSE-tg and control mice.

In summary, despite the chronic overexpression of heparanase, leading to a ~5-fold decrease of glycosaminoglycan-associated anionic sites in the GBM, HPSE-tg mice show a normal renal function and architecture without development of severe albuminuria.

DISCUSSION

In recent years it has been shown that in several (experimental) proteinuric diseases heparanase is upregulated, which was

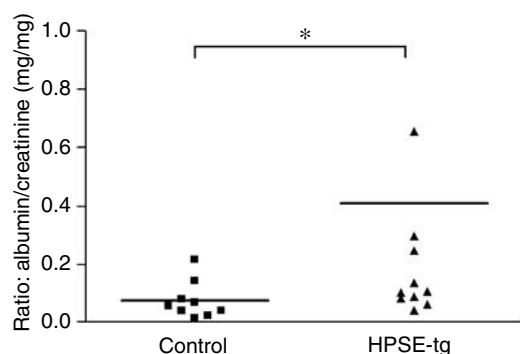


Figure 5 | Urinary albumin/creatinine ratios in HPSE-tg and control mice. In HPSE-tg mice, only a mild but significant increase in urinary albumin excretion could be detected using radial immunodiffusion. However, the majority of HPSE-tg mice showed a normal albumin/creatinine ratio; * $P < 0.05$.

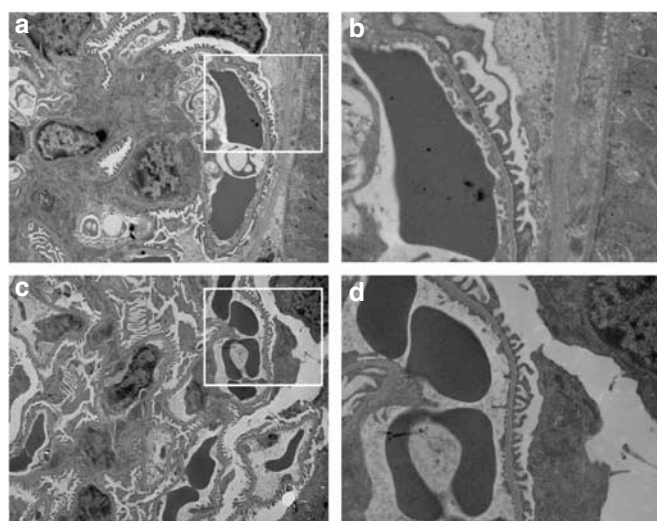


Figure 6 | Glomerular ultrastructure of HPSE-tg and control mice. A normal architecture of the glomerular filtration barrier was observed in all kidney tissue sections of control mice (a, b) and HPSE-tg mice (c, d). Original magnification $\times 5000$ (a, c); original magnification $\times 15000$ (b, d).

associated with a decreased expression of HS in the GBM.^{15–21} It has been postulated that this heparanase-mediated loss of HS in the GBM leads to proteinuria.

In this study we show that chronic and systemic overexpression of heparanase leads to the differential loss of specific HS domains from the GBM. An unmodified *N*-acetylated HS precursor domain (NAH46) and one sulfated HS domain (AO4B08) persisted, whereas another sulfated domain persisted partially (HS4C3). Moreover, this differential loss of HS domains was similar in several tissues, that is, kidney, spleen, and liver. Heparanase only cleaves at specific positions within one HS chain, which results in small HS fragments of different sizes.^{25,37,38} Three different explanations can be postulated for the differential loss of HS domains after heparanase cleavage. First, the HS domains

that (partially) persist may be present in the remnants of HS chains that remain bound to the core protein after cleavage by heparanase, and which do not contain sites susceptible to cleavage by heparanase. Second, the unmodified *N*-acetylated HS domain reflects the first structure after initial HS biosynthesis,¹ whereas the domain defined by antibody AO4B08 may be the first sulfated HS domain arising. Indeed, biochemical analysis of HS of the whole liver and kidney of HPSE-tg mice revealed two to threefold shortened HS chains, which were relative highly 2-*O*-sulfated compared with controls^{27,39} (and JP Li *et al.*, unpublished observations). So, the continuous action of heparanase may lead to trimmed HS chains consisting of HS domains that do not contain sites susceptible to cleavage by heparanase. However, we showed no significant higher urinary secretion of HS in HPSE-tg mice or glomerular intracellular accumulation of sulfated HS, making this option less likely. Third, but less likely, the existence of a subgroup of native HS chains solely consisting of *N*-acetylated domains defined by NAH46 and sulfated domains defined by AO4B08 and/or HS4C3 (Figure 7).

We showed the loss of HS domains with *N*-unsubstituted glucosamine residues in the GBM of patients with overt diabetic nephropathy, which was associated with an increased glomerular expression of heparanase.²⁰ In agreement with our current findings, we also could show that the expression of unmodified *N*-acetylated HS domains in the GBM of diabetic patients was similar to healthy controls (Wijnhoven *et al.*, submitted). The ratio of expression of HS domains with *N*-unsubstituted glucosamine residues (JM403) versus unmodified *N*-acetylated HS domains (NAH46) in the GBM, may be a measure for the glomerular activity of heparanase, which most likely is distinct from other mechanisms leading to loss of HS in the GBM during proteinuric diseases.⁴⁰

In a first inventory of HPSE-tg mice, we observed a mild level of proteinuria.²⁷ Since this could be explained by the presence of the sulfated HS domains defined by AO4B08 and HS4C3 in the GBM of HPSE-tg mice as we show now, we measured the total content of glycosaminoglycan-associated anionic sites in the GBM. Probing with the cationic dye cupromeronic blue revealed a fivefold reduction of glycosaminoglycan-associated anionic sites in the GBM of HPSE-tg mice. The staining of the GBM by AO4B08 is weak in the GBM of both HPSE-tg and control mice, whereas the staining of the GBM by HS4C3 is strongly reduced in the GBM of HPSE-tg mice. Nevertheless, the sulfated HS domains defined by AO4B08 and HS4C3 may be responsible for the remaining glycosaminoglycan-associated anionic sites in the GBM of HPSE-tg mice, as revealed by cupromeronic blue staining. Assessment of renal function, by measuring serum creatinine levels, albuminuria, and glomerular ultrastructure of the mice used for HS analysis, revealed only a marginal, although statistically significant, level of albuminuria. Furthermore, renal function of HPSE-tg mice was normal and glomerular architecture of HPSE-tg mice and controls was similar. In our first inventory, we also found a normal renal function in HPSE-tg mice, but then we had the impression that there was

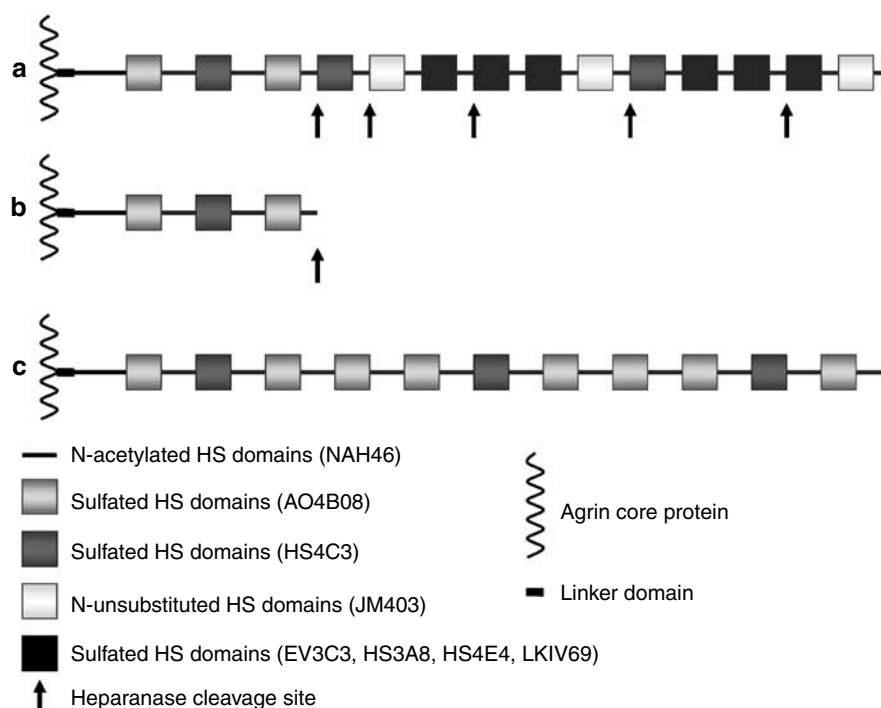


Figure 7 | Possible explanations for the differential loss of HS domains observed after cleavage by heparanase. A differential loss of HS domains was observed after *in vivo* and *in vitro* cleavage of HS by heparanase, which may be explained by three different possibilities.

(a) Unmodified N-acetylated domains (NAH46) and the sulfated domains recognized by AO4B08 may be remnants of HS after cleavage by heparanase and are close to the core protein. The epitope defined by HS4C3 is not fully resistant to heparanase cleavage and is therefore strongly decreased but not absent, whereas the N-unsubstituted domains, recognized by JM403, and the sulfated domains defined by EV3B2, HS3A8, HS4E4, and LKIV69 are lost after degradation of HS by heparanase. (b) HS biosynthesis is not sufficient due to constant trimming of the HS chains by the continuous action of heparanase in HPSE-tg mice, yielding the unmodified N-acetylated HS domains (NAH46) and the sulfated HS domains (AO4B08) that are not susceptible to heparanase cleavage. HS chains may be modified due to constant degradation by heparanase. Only the unmodified N-acetylated HS domains (NAH46) and the AO4B08 domains can be synthesized and are resistant to cleavage by heparanase. (c) Native HS chains exist that solely consist of N-acetylated domains and sulfated domains as defined by AO4B08 are resistant to cleavage by heparanase, since they lack cleavage sites.

a diffuse local podocyte foot process effacement in HPSE-tg mice,²⁷ but this was not substantiated in the current stock of mice. This may be explained by further inbreeding of the HPSE-tg mice in the C57BL/6 background, whereas it is important to stress that foot process effacement and proteinuria not always have to correlate.⁴¹ Nevertheless, we show that glomerular overexpression of heparanase, which is relevant for several (experimental) glomerular diseases,^{15–21} does not lead to significant albuminuria despite the ~5-fold loss of glycosaminoglycan-associated anionic sites in the GBM. These data question the primary role of HS in the GBM in determining the charge-selective properties of the capillary filter. Furthermore, maturation and morphology of podocytes, glomerular endothelium, and mesangium appear not to be influenced by the lack of the majority of HS in the GBM and other glomerular structures.

Recently, other studies also questioned the primary role of HS in the GBM in charge-selective filtration. Mice with podocytes lacking agrin did not develop proteinuria nor revealed an aberrant glomerular architecture.⁴² Mice with podocytes lacking the HS polymerase EXT1 did develop glomerular ultrastructural abnormalities and podocyte loss during the first 8 months, whereas a mild albuminuria

became evident at an age of 8 months.⁴¹ Rats injected with the bacterial HS-degrading enzyme heparinase III, leading to the nearly complete loss of glycosaminoglycan-associated anionic sites in the GBM, did not develop albuminuria within the observation period of 48 h.²² Mice deficient in perlecan and/or collagen XVIII, HS proteoglycan core proteins, mainly expressed in the mesangium and Bowman's capsule, also did not develop glomerular abnormalities and albuminuria under physiological conditions.^{43,44}

Although our current study differs in the approach from the studies mentioned above, fundamentally, they all exclude a primary role of HS in charge-selective filtration. However, in our opinion, we can still not exclude a role for glomerular expression of heparanase and loss of HS in the GBM in the development of proteinuria. We propose two possible mechanisms that are compatible with the current data. In the first sequential mechanism, the heparanase-mediated release of HS fragments or HS-bound factors from the GBM in a situation with glomerular pathology may induce processes leading to or enhancing proteinuria. This pathway is not established in the HPSE-tg, podocyte-specific agrin- and EXT1-deficient mice, since chronic constitutive absence of HS in the GBM under physiological conditions does not

allow the binding of such growth factors or inflammatory mediators and subsequent release of HS fragments or HS-bound factors. The 48-h period as tested for healthy rats injected with heparinase III may have been too short to execute the pathological processes induced by the release of HS fragments or HS-bound factors. In the absence of a proinflammatory microenvironment, HS loss does not lead to pathological consequences. In other words, a single hit is not sufficient for development of proteinuria. Second, assuming such a multi-hit mechanism, the heparanase-mediated loss of HS in the GBM in combination with additional pathological events/signals, like for example local production of angiotensin II, ROS or cytokines, may lead to activation of glomerular cells and development of proteinuria. In all studies mentioned above, only one signal was manipulated, that is, the loss of HS in the GBM. Although our study closely resembles the actual situation of various glomerular diseases by forcing heparanase-mediated HS loss in the GBM, this occurs under non-pathogenic conditions. See van den Hoven *et al.*²¹ for additional discussion on this issue.

That heparanase activity has relevance for development of proteinuria can be derived from earlier studies, which revealed that specific inhibition of heparanase in a proinflammatory situation, like passive Heymann nephritis and experimental anti-GBM nephritis, significantly reduced the development of proteinuria.^{17,45} More definitive studies are required to elucidate the role of heparanase and HS in the development of proteinuria. Proof for this assumption of a multi-hit genesis of proteinuria has to come from experimentally induced glomerular diseases in different models, in which heparanase or HS expression is manipulated. In this respect, induction of proteinuria by, for example, streptozotocin in HPSE-tg mice, in HPSE-deficient mice, or in mice with HPSE-, agrin- or EXT1-deficient podocytes, definitely will give more insight in the importance of heparanase-mediated loss of HS in the pathogenesis of proteinuria.

MATERIALS AND METHODS

Transgenic heparanase-overexpressing mice

HPSE-tg and control mice with a mixed background (C57BL/6 (90–95%) and BALB/c (5–10%)) were generated and genotyped as described.²⁷ Kidney tissue, urine, and serum were obtained from 3- to 12-month-old mice. The housing and handling of the animals were approved by the local animal ethics committees.

Analysis of creatinine, albumin and HS in urine and blood samples

Urinary and serum creatinine were measured enzymatically (Roche Diagnostics, Penzberg, Germany). Serum creatinine was used as a measure for renal function. Urinary albumin was measured by radial immunodiffusion,^{12,46} using goat antiserum against mouse albumin⁴⁷ and purified mouse albumin (Sigma, Zwijndrecht, The Netherlands) as a standard. Urinary albumin excretion was expressed as the ratio mg albumin/mg creatinine. The presence of glycosaminoglycans in the urine was determined after separating urinary glycosaminoglycans by agarose gel electrophoresis followed by a combined azure A-silver staining.⁴⁸

RNA isolation, reversed transcription, and PCR

Total RNA was extracted from renal cortex using the RNeasy mini-kit (Qiagen Benelux, Venlo, The Netherlands). cDNA was prepared by reverse transcription of 1 µg RNA using oligo(dT) primers (Invitrogen, Breda, The Netherlands). Heparanase cDNA was amplified with primers specific for the human heparanase gene. Forward primer (F): 5'-caagaaggaatcaacctttgaag-3', Reversed primer (R): 5'-gtagtccaggagcaactgag-3' using platinum polymerase chain reaction Supermix (Invitrogen). The expression of mouse β-actin was included as a control; F: 5'-gtggcgctctaggaccaa-3', R: 5'-ctctttgatgacgacgatttc-3'. Polymerase chain reaction conditions were as follows: denaturation at 95°C for 3 min, followed by 40 cycles of 95°C for 15 s, 57°C for 30 s, and 72°C for 30 s, and finally elongation at 72°C for 10 min. Polymerase chain reaction products were separated on a 2% agarose gel and visualized with ethidium bromide.

Western blot analysis

Renal cortex was dissolved in lysis buffer containing 50 mM Tris-HCl (pH 8), 150 mM NaCl, 0.5% Triton X-100 (Sigma), and ethylenediamine tetraacetic acid-free protease inhibitors (Roche Almere The Netherlands). Heparanase was concentrated by incubating equal amounts of total protein overnight at 4°C with heparin-agarose beads (Sigma).²⁴ The beads were washed twice in phosphate-buffered saline (PBS), boiled in Laemmli sample buffer, and resolved by sodium dodecyl sulfate-polyacrylamide gel electrophoresis. Proteins were transferred to a polyvinylidene difluoride membrane (Bio-Rad Veenendaal The Netherlands). Blots were blocked with 1% Boehringer blocking reagent (Roche) in PBS. Heparanase was detected by incubation with rabbit polyclonal antibody HPA1 (1:700; ProsPecTany Technogene, Rehovot, Israel) followed by a goat anti-rabbit peroxidase-conjugated antibody (1:8000; Santa Cruz Heer Hugo Waard, The Netherlands). Heparanase protein was visualized using enhanced chemiluminescence reagent (Perbio Science, Etten-Leur, The Netherlands) and ECL hyperfilm (Amersham Biosciences, Buckinghamshire, UK).

Antibodies, immunofluorescence staining, and treatment with active heparanase

The expression of different HS domains, chondroitin sulfate, dermatan sulfate, agrin core protein, and heparanase was detected by specific antibodies as listed in Table 1. The phage display-derived single-chain antibodies (scFv) were prepared as described.^{32,30,33} Mouse kidney sections were fixed in acetone for 10 min at 4°C and then incubated for 1 h at room temperature with primary antibodies. For monoclonal mouse antibodies, sections were first blocked using the mouse-on-mouse kit (Vector Laboratories Inc., Burlingame, CA, USA). Sections were washed with PBS and incubated with secondary antibodies for 1 h at room temperature. The scFv antibodies were detected by the rabbit anti-Vesicular Stomatitis Virus (VSV) antibody (1:500; MBL, Nagoya, Japan). The mouse IgM antibodies, hamster IgG antibody, and rabbit IgG antibodies were, respectively, detected by goat anti-mouse IgM Alexa 488 (1:200; Invitrogen), goat anti-hamster fluorescein isothiocyanate (1:400; MP Biomedicals, Eschwege, Germany) and goat anti-rabbit IgG Alexa 488 (1:200; Invitrogen). All antibodies were diluted in PBS supplemented with 2% (w/v) bovine serum albumin and 0.05% (v/v) Tween-20 (Sigma). Normal goat serum (4%) was added to all secondary antibodies. Finally, sections were washed in PBS, embedded in Vectashield mounting medium H-1000 (Vector Laboratories Inc.), and examined with a Zeiss Axioskop microscope (Carl Zeiss BV, Sliedrecht, The Netherlands).

To mimic the effect of *in vivo* heparanase overexpression *in vitro*, renal cryosections of normal mice were incubated with active recombinant human heparanase ($0.22 \mu\text{g ml}^{-1}$) in 50 mM sodium acetate buffer (pH 5) for 2 h at 37°C . Then, sections were washed in PBS, fixed, and stained as described above.

Digestion of HS by recombinant heparanase in enzyme-linked immunosorbent assay

Flat bottom 96-well plates (Nunc A/S, Roskilde, Denmark) were coated with $5 \mu\text{g}$ per well HS from bovine kidney (Seikagaku, Tokyo, Japan) in PBS overnight at 4°C . Wells were left untreated or incubated with 0.3 or $2.5 \mu\text{g ml}^{-1}$ active recombinant human heparanase in 50 mM sodium acetate buffer (pH 5) for 3 h at 37°C . Plates were washed with PBS with 0.5% Tween and blocked with PBS with 1% gelatin for 1 h. Plates were washed with PBS/Tween and incubated with anti-HS antibodies for 1 h in PBS/gelatin. Dilutions of anti-HS antibodies were chosen from serial dilutions on coated HS that allowed detection of a decrease in HS. Anti-HS antibody binding was detected by incubating with the appropriate horseradish peroxidase-conjugated antibodies in PBS/gelatin for 1 h. Finally, the plates were washed with PBS/Tween and incubated with tetramethylbenzidine solution (SFRI Laboratories, Berganton, France). After 15 min, the reaction was stopped with 2 M H_2SO_4 and absorption was measured at 450 nm.

Visualization of glycosaminoglycan-associated anionic sites by cupromeronic blue staining

Glycosaminoglycan-associated anionic sites were visualized by the critical electrolyte concentration method as described.³⁶ We have shown previously that this staining method is rather specific for HS because heparinase III treatment abolished cupromeronic blue staining in the GBM, whereas staining was not influenced by chondroitinase ABC treatment.^{22,49} Pieces of cortex were fixed for 24 h in 25 mM sodium acetate (pH 5.6) containing 2.5% (v/v) glutaraldehyde, 0.2 M MgCl_2 , and 0.2% (w/v) cupromeronic blue (Seikagaku). Subsequently, tissue was washed three times with fixing solution and three times with water containing 1% (w/v) Na-tungstate. Tissue was dehydrated by sequentially incubating in solutions with increasing concentrations of ethanol containing 1% Na-tungstate. After incubation in 100% ethanol, tissue was incubated in propylene oxide, followed by incubation with 50% (v/v) propylene oxide and Epon for 16 h, and with 100% (v/v) Epon for a subsequent 16 h. Finally, tissue was embedded by sequentially increasing the temperature (37, 45, and 60°C for 24 h each). Ultra-thin sections were prepared and examined with a Jeol TEM 1010 microscope (JEOL, Tokyo, Japan).

Determination of glomerular ultrastructure by transmission electron microscopy

Pieces of cortex were fixed in 2.5% glutaraldehyde dissolved in 0.1 M sodium cacodylate buffer, pH 7.4, for 7 days at 4°C . After washing in cacodylate buffer, tissue was postfixed in palade-buffered 2% OsO_4 for 1 h, dehydrated, and embedded in Epon 812, Luft's procedure (Merck, Darmstadt, Germany). Ultra-thin sections (90 nm) were stained with 4% uranyl acetate for 45 min, followed by lead citrate for 5 min at room temperature. Sections were examined with a Jeol 1200 EX2 electron microscope (JEOL).

Statistical analysis

Significance was evaluated by the non-parametric Mann-Whitney *U*-test using GraphPad Prism 4.0. (GraphPad Software Inc., San Diego, CA, USA). *P*-values ≤ 0.05 were considered statistically significant.

ACKNOWLEDGMENTS

This study was supported by the Dutch Diabetes Research Foundation (grant 2001.00.048), the Dutch Kidney Foundation (grant C05.5152), The Netherlands Organization for Scientific Research (grant 902-27-292), the JDRF (grant 2006-695), and the European Union (grant QLK3-CT-2002-02049).

REFERENCES

1. Esko JD, Selleck SB. Order out of chaos: assembly of ligand binding sites in heparan sulfate. *Annu Rev Biochem* 2002; **71**: 435–471.
2. Turnbull J, Powell A, Guimond S. Heparan sulfate: decoding a dynamic multifunctional cell regulator. *Trends Cell Biol* 2001; **11**: 75–82.
3. Daniels BS. Increased albumin permeability *in vitro* following alterations of glomerular charge is mediated by the cells of the filtration barrier. *J Lab Clin Med* 1994; **124**: 224–230.
4. Kanwar YS, Linker A, Farquhar MG. Increased permeability of the glomerular basement membrane to ferritin after removal of glycosaminoglycans (heparan sulfate) by enzyme digestion. *J Cell Biol* 1980; **86**: 688–693.
5. Kanwar YS, Rosenzweig LJ, Kerjaschki DI. Glycosaminoglycans of the glomerular basement membrane in normal and nephrotic states. *Ren Physiol* 1981; **4**: 121–130.
6. Rosenzweig LJ, Kanwar YS. Removal of sulfated (heparan sulfate) or nonsulfated (hyaluronic acid) glycosaminoglycans results in increased permeability of the glomerular basement membrane to 125I-bovine serum albumin. *Lab Invest* 1982; **47**: 177–184.
7. Miettinen A, Stow JL, Mentone S *et al*. Antibodies to basement membrane heparan sulfate proteoglycans bind to the laminae rarae of the glomerular basement membrane (GBM) and induce subepithelial GBM thickening. *J Exp Med* 1986; **163**: 1064–1084.
8. van den Born J, van den Heuvel LP, Bakker MA *et al*. A monoclonal antibody against GBM heparan sulfate induces an acute selective proteinuria in rats. *Kidney Int* 1992; **41**: 115–123.
9. Raats CJ, Luca ME, Bakker MA *et al*. Reduction in glomerular heparan sulfate correlates with complement deposition and albuminuria in active Heymann nephritis. *J Am Soc Nephrol* 1999; **10**: 1689–1699.
10. Raats CJ, Bakker MA, van den Born J *et al*. Hydroxyl radicals depolymerize glomerular heparan sulfate *in vitro* and in experimental nephrotic syndrome. *J Biol Chem* 1997; **272**: 26734–26741.
11. Tamsma JT, van den Born J, Bruijn JA *et al*. Expression of glomerular extracellular matrix components in human diabetic nephropathy: decrease of heparan sulphate in the glomerular basement membrane. *Diabetologia* 1994; **37**: 313–320.
12. van Bruggen MC, Kramers K, Hykema MN *et al*. Decrease of heparan sulfate staining in the glomerular basement membrane in murine lupus nephritis. *Am J Pathol* 1995; **146**: 753–763.
13. van den Born J, van den Heuvel LP, Bakker MA *et al*. Distribution of GBM heparan sulfate proteoglycan core protein and side chains in human glomerular diseases. *Kidney Int* 1993; **43**: 454–463.
14. Raats CJ, Bakker MA, Hoch W *et al*. Differential expression of agrin in renal basement membranes as revealed by domain-specific antibodies. *J Biol Chem* 1998; **273**: 17832–17838.
15. Levidiotis V, Kanellis J, Ierino FL *et al*. Increased expression of heparanase in puromycin aminonucleoside nephrosis. *Kidney Int* 2001; **60**: 1287–1296.
16. Levidiotis V, Freeman C, Tikellis C *et al*. Heparanase is involved in the pathogenesis of proteinuria as a result of glomerulonephritis. *J Am Soc Nephrol* 2004; **15**: 68–78.
17. Levidiotis V, Freeman C, Tikellis C *et al*. Heparanase inhibition reduces proteinuria in a model of accelerated anti-glomerular basement membrane antibody disease. *Nephrology (Carlton)* 2005; **10**: 167–173.
18. Kramer A, van den Hoven M, Rops A *et al*. Induction of glomerular heparanase expression in rats with adriamycin nephropathy is regulated by reactive oxygen species and the renin-angiotensin system. *J Am Soc Nephrol* 2006; **17**: 2513–2520.
19. Maxhimer JB, Somenek M, Rao G *et al*. Heparanase-1 gene expression and regulation by high glucose in renal epithelial cells: a potential role in the pathogenesis of proteinuria in diabetic patients. *Diabetes* 2005; **54**: 2172–2178.
20. van den Hoven MJ, Rops AL, Bakker MA *et al*. Increased expression of heparanase in overt diabetic nephropathy. *Kidney Int* 2006; **70**: 2100–2108.
21. van den Hoven MJ, Rops AL, Vlodavsky I *et al*. Heparanase in glomerular diseases. *Kidney Int* 2007; **72**: 543–548.

22. Wijnhoven TJ, Lensen JF, Wismans RG *et al.* *In vivo* degradation of heparan sulfates in the glomerular basement membrane does not result in proteinuria. *J Am Soc Nephrol* 2007; **18**: 823–832.
23. Ilan N, Elkin M, Vlodavsky I. Regulation, function and clinical significance of heparanase in cancer metastasis and angiogenesis. *Int J Biochem Cell Biol* 2006; **38**: 2018–2039.
24. Abboud-Jarrous G, Rangini-Guetta Z, Aingorn H *et al.* Site-directed mutagenesis, proteolytic cleavage, and activation of human proheparanase. *J Biol Chem* 2005; **280**: 13568–13575.
25. Okada Y, Yamada S, Toyoshima M *et al.* Structural recognition by recombinant human heparanase that plays critical roles in tumor metastasis. Hierarchical sulfate groups with different effects and the essential target disulfated trisaccharide sequence. *J Biol Chem* 2002; **277**: 42488–42495.
26. Pikas DS, Li JP, Vlodavsky I *et al.* Substrate specificity of heparanases from human hepatoma and platelets. *J Biol Chem* 1998; **273**: 18770–18777.
27. Zcharia E, Metzger S, Chajek-Shaul T *et al.* Transgenic expression of mammalian heparanase uncovers physiological functions of heparan sulfate in tissue morphogenesis, vascularization, and feeding behavior. *FASEB J* 2004; **18**: 252–263.
28. van den Born J, Jann K, Assmann KJ *et al.* N-acetylated domains in heparan sulfates revealed by a monoclonal antibody against the *Escherichia coli* K5 capsular polysaccharide. Distribution of the cognate epitope in normal human kidney and transplant kidney with chronic vascular rejection. *J Biol Chem* 1996; **271**: 22802–22809.
29. van den Born J, Gunnarsson K, Bakker MA *et al.* Presence of N-unsubstituted glucosamine units in native heparan sulfate revealed by a monoclonal antibody. *J Biol Chem* 1995; **270**: 31303–31309.
30. Jenniskens GJ, Oosterhof A, Brandwijk R *et al.* Heparan sulfate heterogeneity in skeletal muscle basal lamina: demonstration by phage display-derived antibodies. *J Neurosci* 2000; **20**: 4099–4111.
31. Kurup S, Wijnhoven TJ, Jenniskens GJ *et al.* Characterization of anti-heparan sulfate phage-display antibodies AO4B08 and HS4E4. *J Biol Chem* 2007; **282**: 21032–21042.
32. Dennissen MA, Jenniskens GJ, Pieffers M, *et al.* Large, tissue-regulated domain diversity of heparan sulfates demonstrated by phage display antibodies. *J Biol Chem* 2002; **277**: 10982–10986.
33. van Kuppevelt TH, Dennissen MA, van Venrooij WJ *et al.* Generation and application of type-specific anti-heparan sulfate antibodies using phage display technology. Further evidence for heparan sulfate heterogeneity in the kidney. *J Biol Chem* 1998; **273**: 12960–12966.
34. Wijnhoven TJ, Lensen JF, Rops AL *et al.* Aberrant heparan sulfate profile in the human diabetic kidney offers new clues for therapeutic glycomimetics. *Am J Kidney Dis* 2006; **48**: 250–261.
35. Smetsers TF, van de Westerloo EM, ten Dam GB *et al.* Human single-chain antibodies reactive with native chondroitin sulfate detect chondroitin sulfate alterations in melanoma and psoriasis. *J Invest Dermatol* 2004; **122**: 707–716.
36. van Kuppevelt TH, Veerkamp JH. Application of cationic probes for the ultrastructural localization of proteoglycans in basement membranes. *Microsc Res Tech* 1994; **28**: 125–140.
37. Parish CR, Freeman C, Hulett MD. Heparanase: a key enzyme involved in cell invasion. *Biochim Biophys Acta* 2001; **1471**: M99–M108.
38. Vlodavsky I, Goldshmidt O. Properties and function of heparanase in cancer metastasis and angiogenesis. *Haemostasis* 2001; **31**(Suppl 1): 60–63.
39. Li JP, Galvis ML, Gong F *et al.* *In vivo* fragmentation of heparan sulfate by heparanase overexpression renders mice resistant to amyloid protein A amyloidosis. *Proc Natl Acad Sci USA* 2005; **102**: 6473–6477.
40. Raats CJ, van den Born J, Berden JH. Glomerular heparan sulfate alterations: mechanisms and relevance for proteinuria. *Kidney Int* 2000; **57**: 385–400.
41. Chen S, Holzman L, Yamaguchi Y *et al.* Elimination of heparan sulfate glycosaminoglycans (HS-GAGs) from the glomerular basement membrane (GBM) using Cre-Lox technology has profound effect on podocyte ultrastructure and function [Abstract]. *J Am Soc Nephrol* 2006; **17**: 25A.
42. Harvey SJ, Jarad G, Cunningham J *et al.* Disruption of glomerular basement membrane charge through podocyte-specific mutation of agrin does not alter glomerular permselectivity. *Am J Pathol* 2007; **171**: 139–152.
43. Morita H, Yoshimura A, Inui K *et al.* Heparan sulfate of perlecan is involved in glomerular filtration. *J Am Soc Nephrol* 2005; **16**: 1703–1710.
44. Rossi M, Morita H, Sormunen R *et al.* Heparan sulfate chains of perlecan are indispensable in the lens capsule but not in the kidney. *EMBO J* 2003; **22**: 236–245.
45. Levidiotis V, Freeman C, Punler M *et al.* A synthetic heparanase inhibitor reduces proteinuria in passive Heymann nephritis. *J Am Soc Nephrol* 2004; **15**: 2882–2892.
46. Assmann KJ, Tangelder MM, Lange WP *et al.* Anti-GBM nephritis in the mouse: severe proteinuria in the heterologous phase. *Virchows Arch A Pathol Anat Histopathol* 1985; **406**: 285–299.
47. Assmann KJ, Tangelder MM, Lange WP *et al.* Membranous glomerulonephritis in the mouse. *Kidney Int* 1983; **24**: 303–312.
48. van de Lest CH, Versteeg EM, Veerkamp JH *et al.* Quantification and characterization of glycosaminoglycans at the nanogram level by a combined azure A–silver staining in agarose gels. *Anal Biochem* 1994; **221**: 356–361.
49. van den Born J, van Kraats AA, Bakker MA *et al.* Reduction of heparan sulphate-associated anionic sites in the glomerular basement membrane of rats with streptozotocin-induced diabetic nephropathy. *Diabetologia* 1995; **38**: 1169–1175.